Volume 19, Issue 2, 192525 (1-8)

Majlesi Journal of Electrical Engineering (MJEE)

https://doi.org/10.57647/j.mjee.2025.1902.25

A multi-band spiral-shaped patch CPW-fed CP antenna

Loghman Asadpor*

Department of Electrical Engineering, Urmia Branch, Islamic Azad University, Urmia, Iran.
Microwave and Antenna Research Center, Urmia Branch, Islamic Azad University, Urmia, Iran.

*Corresponding author: loghman.asadpour@iau.ac.ir

Original Research

Received:
15 March 2025
Revised:
2 May 2025
Accepted:
10 May 2025
Published online:
1 June 2025

Abstract:

A miniaturized quadruple-band antenna with a spiral-shaped patch is proposed to cover wireless system bands including GSM, Wi-Fi/WLAN (IEEE 802.11b/g/n), Extended UMTS (IEEE 802.11y), WiMAX and the Wi-Fi/WLAN2 (IEEE 802.11a/h/j). The antenna design features a CPW-fed configuration with a spiral-shaped patch, vertical slot, and open-end slits in a rectangular ground plane. In the design of this antenna, the POES structure is used to improve the characteristics of the antenna. A prototype antenna was constructed and tested, demonstrating operation across four frequency bands ranging from 1.71 GHz to 7.1 GHz. The antenna exhibits circular polarization, a monopole like radiation pattern, and good gain over its operating bands, making it suitable for GSM, Extended UMTS, WiMAX, and Wi-Fi/WLAN applications. The antennas overall dimension is 27×25 mm^2.

Keywords: Spiral shaped antenna; Defected ground structure; Periodic open-end slit; WiMAX/Wi-Fi/WLAN; Circular polarization

1. Introduction

The increasing demand for multiband antennas is driven by the need to integrate multiple communication standards into compact systems for enhanced portability of personal communication devices. Popular multiband antennas, such as planar and coplanar monopoles, offer advantages like low profile, lightweight design, and cost-effectiveness. However, designing compact antennas for multiple frequency bands remains a challenge. Various feed structures, including probe [1–5], microstrip [6–9] and coplanar waveguide [10–14] (CPW), have been utilized to address this challenge. Additionally, defected ground structure (DGS) has emerged as a promising method to reduce antenna size and enhance resonance modes [15–19]. During the study process, the articles in which the antennas with optimal performance in obtaining the circular polarization characteristic and using the coplanar feed line were also used [20, 21]. It should be noted that in some sources, this feature was obtained using the array antenna method [22, 23], but due to the high gain of these antennas, they had a complex structure, which is considered one of their disadvantages.

In this study, a small multiband CPW-fed monopole antenna is proposed for GSM, Extended UMTS, WiMAX, and Wi-Fi/WLAN applications. The antenna provides four distinct impedance bandwidths across different frequency ranges. It features a spiral shaped patch with a vertical slot and open-end slits in the ground plane, optimized using Ansoft's HFSS software. Practical measurements confirm the antenna's circular polarization, monopole like radiation pattern, and good gain over its operating bands, all within a compact size of 27×25 mm^2.

2. Technical work preparation

The CPW-fed monopole antenna with a spiral-shaped patch is depicted in Fig. 1. The antenna structure is etched on a PCB with specific dimensions and material properties. The antenna parameters were optimized using HFSS software. The antenna uses a CPW-fed tapered patch for excitation and has a characteristic impedance of 50 Ω, terminated with an SMA connector. In the design of the presented antenna, a relatively new structure called POES (periodic open-end stubs) is used. The POES structure used around the feed line and on the ground plane creates good impedance matching, and this itself creates an impedance bandwidth, and on the other hand, with the proper distribution of surface currents, the co-pol gets bigger and the cross-pol gets smaller. As we know for circular polarization, the co-polarization difference (also known as axial ratio) should ideally be close

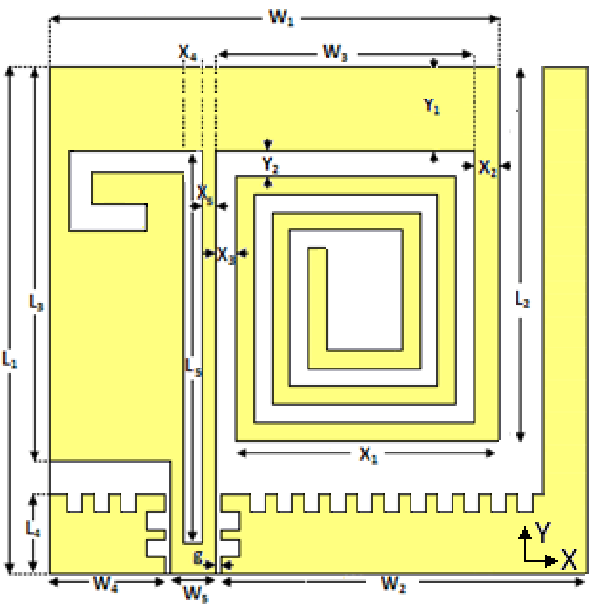

$L_1 = 27.00$ mm	$W_2 = 18.15$ mm	$X_3 = 1.15$ mm
$L_2 = 17.60$ mm	$W_3 = 14.35$ mm	$X_4 = 1.00$ mm
$L_3 = 20.75$ mm	$W_4 = 6.45$ mm	$X_5 = 0.75$ mm
$L_4 = 4.40$ mm	$W_5 = 2.50$ mm	$Y_1 = 1.50$ mm
$L_5 = 21.87$ mm	$X_1 = 14.60$ mm	$Y_2 = 1.40$ mm
$W_1 = 25.00$ mm	$X_2 = 1.40$ mm	$g = 0.30$ mm

Figure 1. Geometry of the proposed multi-band antenna along with the table of physical parameters.

to 0 dB, indicating that the two orthogonal components of the circularly polarized wave have equal amplitudes. The cross-polarization difference should be as low as possible, typically less than -10 dB, to ensure good circular polarization purity.
The fabrication of the antenna is straightforward as it requires only one layer of substrate with metallization due to the feeding structure and antenna being on the same plane. The antenna design includes a spiral strip with specific dimensions. The VSWR of the antenna was measured using a Vector Network Analyzer. The evolution of the antenna design and its reflection coefficient response are shown in Fig. 3.
The simulation results for Antenna (a) reveal three resonant bands, with the first band having a weak reflection coefficient. The second band operates from $3.30-4.02$ GHz, covering Wi-Fi/WLAN (IEEE 802.11y: $3.650-3.700$ GHz), and the third band spans $4.41-7.4$ GHz, encompassing Wi-Fi/WLAN (IEEE 802.11a/h/j: $5.150-5.825$ GHz). Antenna (b) extends the spiral to excite four resonance modes covering various frequency ranges, including GPS and Extended UMTS. Antenna (c) further extends the spiral, generating four frequency bands across different ranges. The inclusion of a vertical slot and open-end slits near the feed-line improves the antenna's reflection coefficient and impedance bandwidth, as depicted in Fig. 4. Table 1 lists the corresponding simulated data for all antennas. The spiral structure enables the creation of a multi-band antenna without increasing its overall dimensions. The optimized open-end slits are 1×1 mm^2 in size and located 1 mm from the top and bottom of the ground plane.

3. Results and discussion

Increasing the length of spiral strips in microstrip antennas can have different effects on the impedance bandwidth of the antenna. These effects depend on other factors such as the shape and dimensions of the spiral strips, the number of spiral turns and the frequency of antenna operation. However in general, increasing the length of the spiral strips may lead to an increase in the impedance bandwidth of the antenna. By increasing the length of the spiral strips, the response frequencies of the antenna also increase and this increases the impedance bandwidth. Increasing the number of spiral turns, can also help to increase the impedance bandwidth. Therefore, increasing the length of spiral strips can lead to an increase in the impedance bandwidth of microstrip antennas. The impact of spiral width on the multi-band performance was studied, with simulation results depicted in Fig. 5. A spiral width of 0.7 mm generated four resonance modes, albeit with a weak first mode, occurring at 2.55, 3.60, and 5.57 GHz. Similarly, a spiral width of 1.3 mm also produced four resonance modes within comparable frequency bands, highlighting an optimal value of 1 mm for the spiral strip width. The reflection coefficient results for the proposed antenna, as illustrated in Fig. 5, demonstrate four impedance bands with 10-dB reflection coefficients spanning frequency ranges of $1.71-1.94$ GHz, $2.35-2.7$ GHz, $3.09-3.87$ GHz, and $4.44-7.20$ GHz, meeting the band-

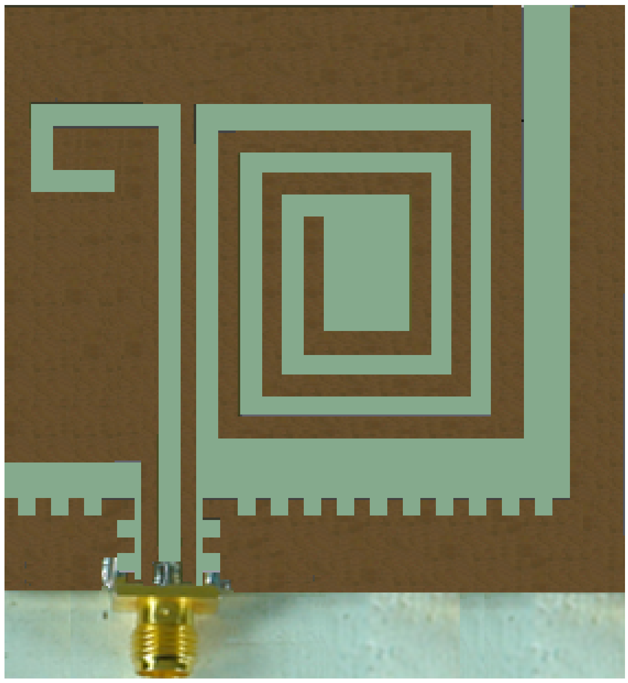

Figure 2. Fabricated antenna.

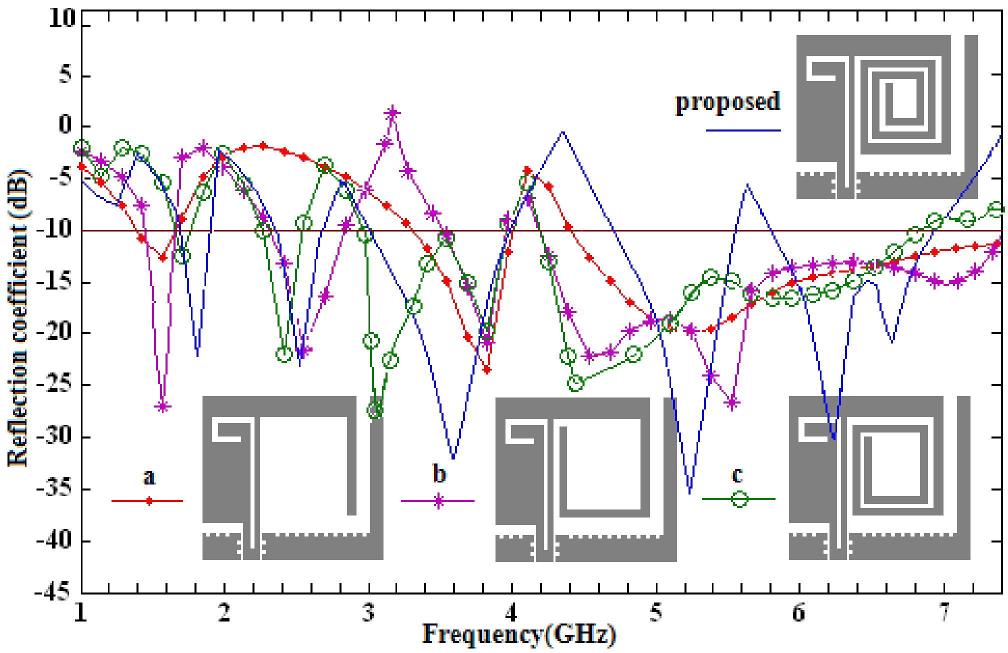

Figure 3. Design evolution of the proposed antenna and the corresponding reflection coefficient characteristics.

width requirements of GSM, Extended UMTS, WiMAX, and Wi-Fi/WLAN. Additionally, a weak resonant mode at 1.30 GHz was observed. The surface currents distribution and the surface current densities distribution at the four modes are visualized in Fig. 7.

Surface currents in the antenna represent the electric current that flows on the surface of the antenna. These currents are important for the propagation and radiation of electromagnetic waves. Surface currents are created due to the effects of the electromagnetic field and changes in the electric current on the surface of the antenna. The surface currents in the antenna produce the magnetic field and the electric field required for the radiation of electromagnetic waves. These currents transfer energy to electromagnetic waves and transfer information to space. In general, the surface currents in the antenna play a very important role in the performance and efficiency of the antenna and must be properly managed to maintain the optimal performance of the antenna.

At the first mode (1.85 GHz), the current is concentrated on the left-hand side of the spiral strip, near the vertical slot and open-end slits. For the second mode (2.55 GHz), the current is prominent on the right side of the spiral and

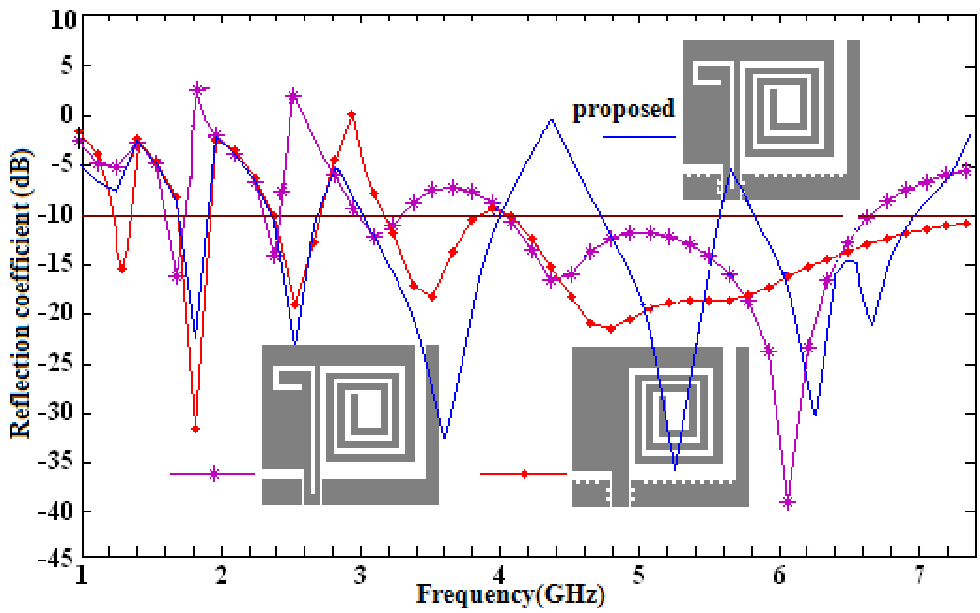

Figure 4. The effect on the antenna's reflection coefficient with and without of (i) the vertical slot in the patch, and (ii) ground-plane open-end slits.

Table 1. Related simulation data for all of antennas.

Key parameters	BW F_{lower} ~f_{higher} GHz	BW (%)	GSM	Wi-Fi/WLAN (IEEE 802.11 b/g/n)	UMTS	Wi-Fi/WLAN (IEEE 802.11 y)	Wi-Fi/WLAN2 (IEEE 802.11 a/h/j)
Antenna (a)	3.30-4.02 4.41-7.4	100 100	×	×	×	✓	✓
Antenna (b)	1.46-1.67 2.31-2.81 3.52-3.96	100 100 90	✓	×	✓	✓	×
Antenna (c)	2.27-2.55 2.95-3.60 3.60-3.96 4.20-6.8	65 0 100 100	×	×	✓	✓	✓
Proposed Antenna	1.71-1.95 2.40-2.75 3.18-3.62 4.45-5.31 5.81-7.12	75 100 100100 85	✓	✓	✓	✓	✓

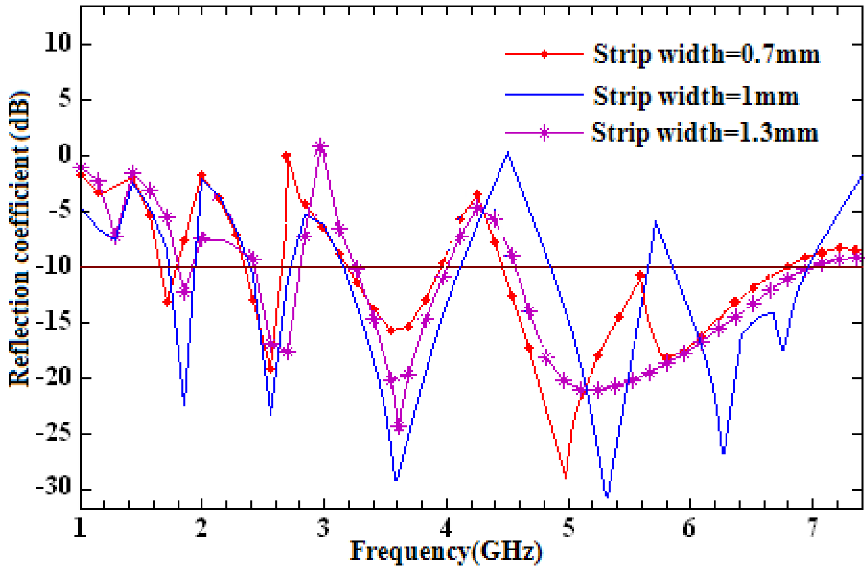

Figure 5. Effect on the reflection coefficient as a function of the spiral strip width.

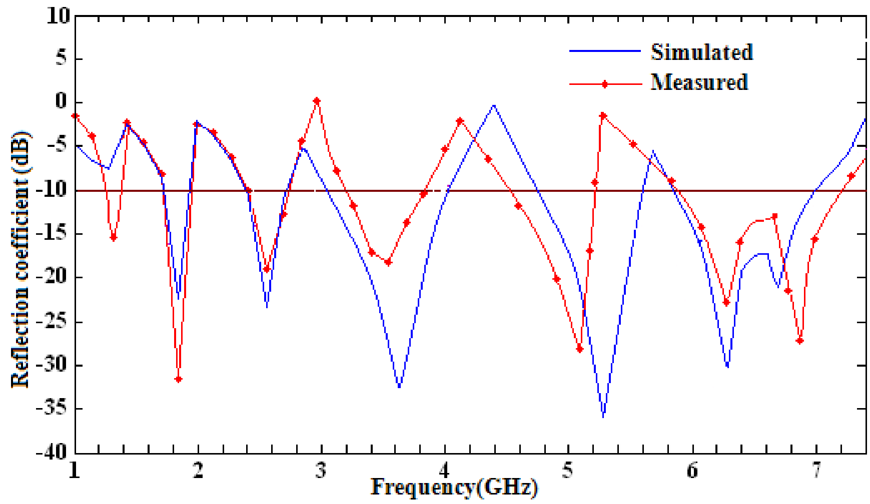

Figure 6. Simulated and measured reflection coefficient of the proposed antenna.

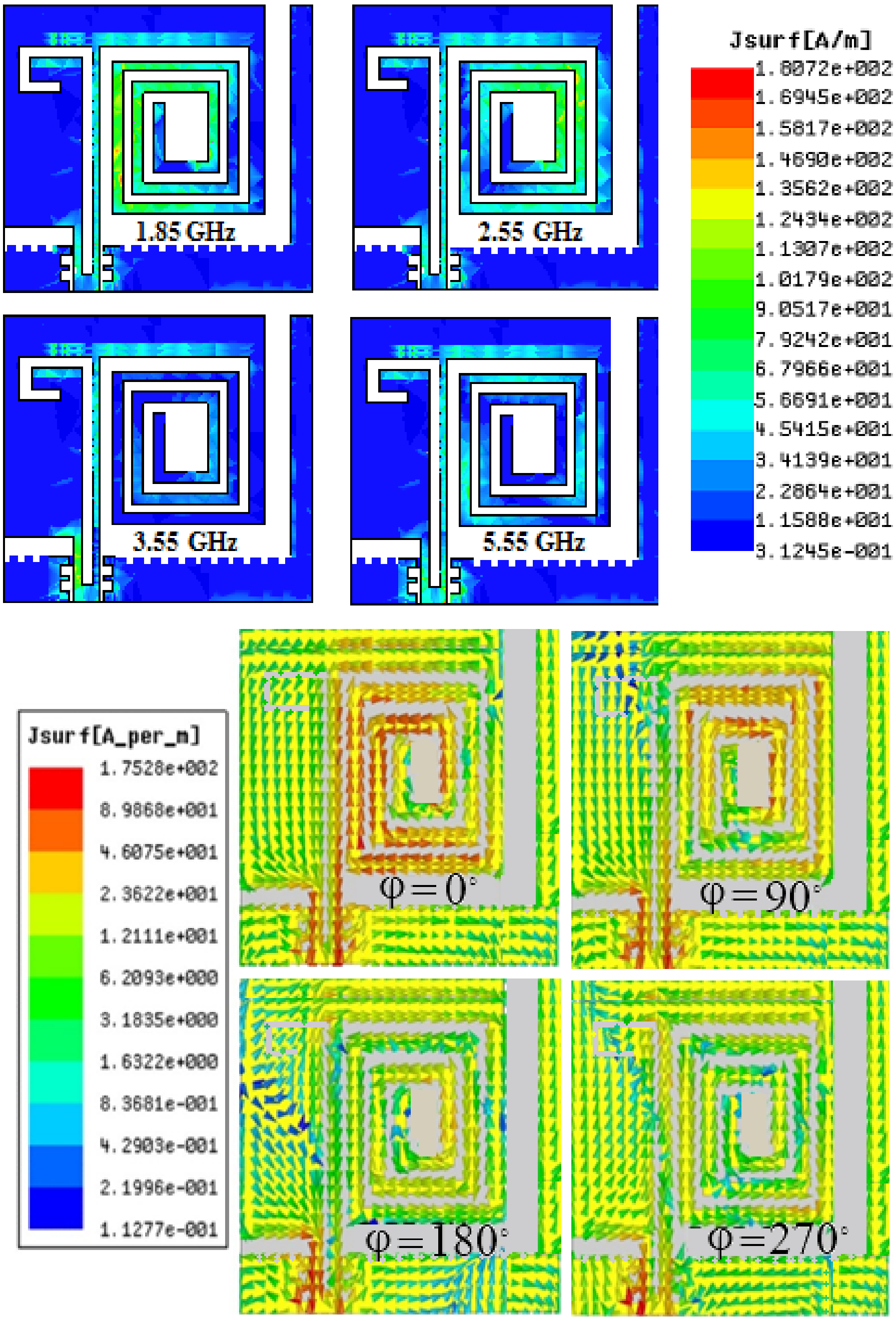

Figure 7. (a): Surface currents distribution and (b): Surface current densities distribution.

around the vertical slot and open-end slits. At the third resonance mode (3.55 GHz), the current is strong around the open-end slits and near the center of the spiral, while for the fourth mode (5.55 GHz), the current distribution primarily surrounds the spiral except at its center. These current density patterns offer insights into the regions of the patch influencing the resonance bands.
The radiation patterns at the four resonance bands in both the x-z plane (E-plane) and y-z plane (H-plane) were compared in Fig. 8. The antenna's radiation properties remain consistent across its operational frequencies, with minimal cross-polarization effects. It is important to highlight that all radiation patterns were measured in the broadside direction. To achieve circular polarization, a current rotating technique was employed in designing the spiral patch, introducing a 90-degree phase shift between the surface current along the radiation patch slits. This led to current distortion in different areas of the patch, enabling circular polarization. According to the explanations given, because the phase at angle between the electric field and the magnetic field in this antenna is almost equal to 90 degrees, circular polarization is of type LHCP in this antenna. In the left-hand circular polarization, the electric field and the magnetic field are circular. They move and their direction of rotation is clockwise. Left-handed circular polarization leads to the production of linear wave's perpendicular to the plane of radiation, which are used in many applications. This type of polarization plays a role in the transmission of energy and

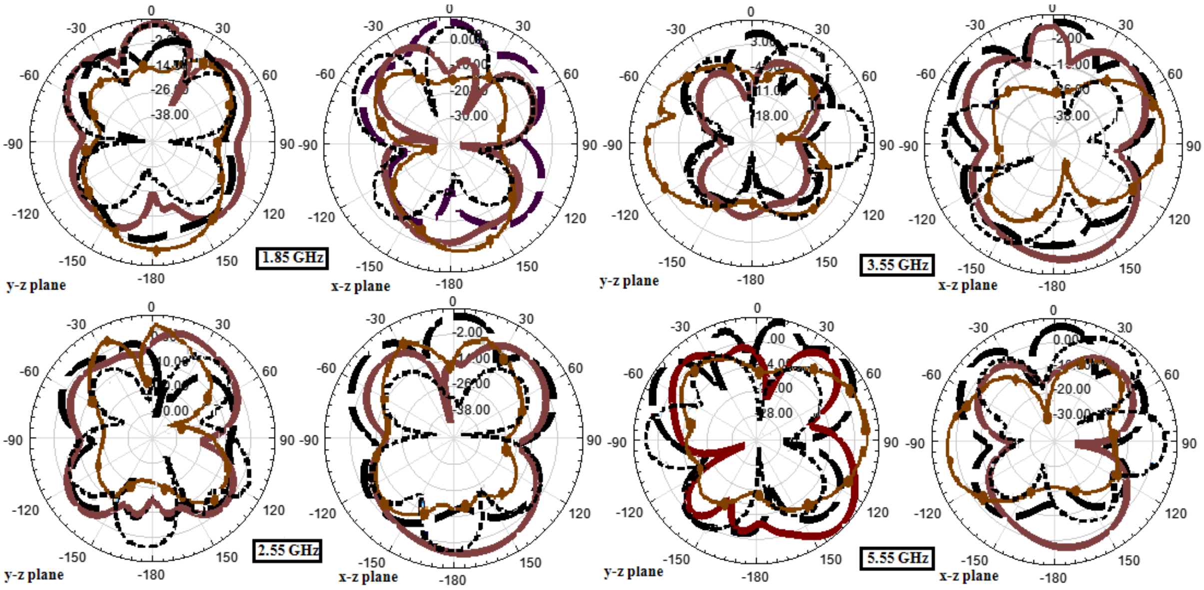

Figure 8. Simulated & Measured radiation patterns of the antenna at 1.85, 2.55, 3.55 and 5.5 GHz in the x-z plane and y-z plane.

information in electromagnetic waves. It is important and is used to transmit information optimally. In general, left-handed circular polarization is a special and useful type of polarization in the science of electromagnetics and wireless communication, which has its own unique characteristics. The axial-ratio simulations at the four frequency bands illustrated in Fig. 9 confirm the antenna's circular polarization capabilities across all bands. In this antenna, the radiation patterns are measured in the broadside direction, while the directions in which the circular polarization characteristic was obtained were not in the broadside as mentioned in figure 9. Additionally, in this antenna with a spiral patch design, we used the current rotation technique and were able to create a 90-degree phase difference between the surface current along the gaps of the radiation patch and to create current distortion in different areas on the patch, resulting in the characteristic of left-handed circular polarization being obtained. The antenna's ability to support the full rotation of surface current flow contributes to this characteristic, as demonstrated by the comparison with band widths and axial ratio values provided in Table 2.The gain performance of the multi-band antenna, as simulated and

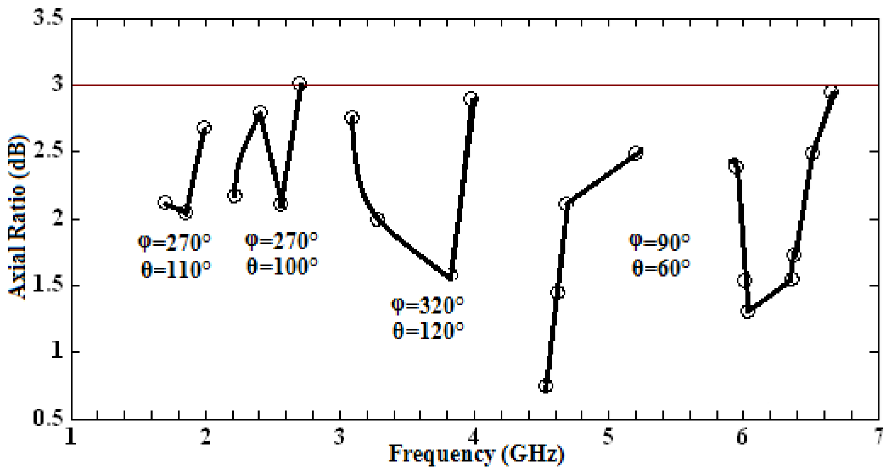

Figure 9. Simulated Axial-ratio of the proposed antenna as a function of frequency.

Table 2. Comparison with the received band widths and obtained axial ratio.

Reflection Coefficient BW (GHz)	1.71-1.95	2.40-2.75	3.18-3.62	4.45-5.31	5.81-7.12
Axial Ratio BW (GHz)	1.71-1.95	2.42-2.75	3.17-4.02	4.25-5.25	3.81-6.62

measured, is displayed in Fig. 10. Within the frequency range of 1.71 – 1.95 GHz, the measured gain varies between 0.55 – 0.80 dB. The second band exhibits a peak gain of 1.42 dB with a gain variation of 1.13 dB. In contrast, the third band's peak gain decreases to 1.95 dB, with a gain variation of 0.85 dB. Lastly, the fourth band showcases a peak gain of 2.75 dB, with a gain variation of approximately 2 dB.

As seen in figure 10, the gain of the antenna depends on the frequency because the size and shape of the antenna are determined based on the signal wavelength and frequency. As the frequency increases, the wavelength decreases, and this causes the size of the antenna to decrease. This reduction in antenna size leads to an increase in antenna gain, as smaller antennas are able to absorb higher frequency signals. In other words, by increasing the frequency, the antenna has more gain and shows better performance. For a better comparison between the provided antenna and some of the mentioned references, Table 3 is provided.

4. Conclusion

A compact multi-band monopole antenna was introduced, covering the GSM, Extended UMTS, WiMAX, and Wi-Fi/WLAN frequency bands. It utilized a spiral-shaped patch design with a vertical slot and open-end slits in the CPW feed line to improve the reflection coefficient and impedance bandwidth. The POES structure used in the antenna, in addition to improving the impedance matching, also result in better radiation performance of the presented antenna. The impact of various physical parameters was studied for further understanding. Practical validation confirmed its suitability for wireless communication due to its compact size, defected ground plane, favorable radiation patterns, and circular polarization properties.

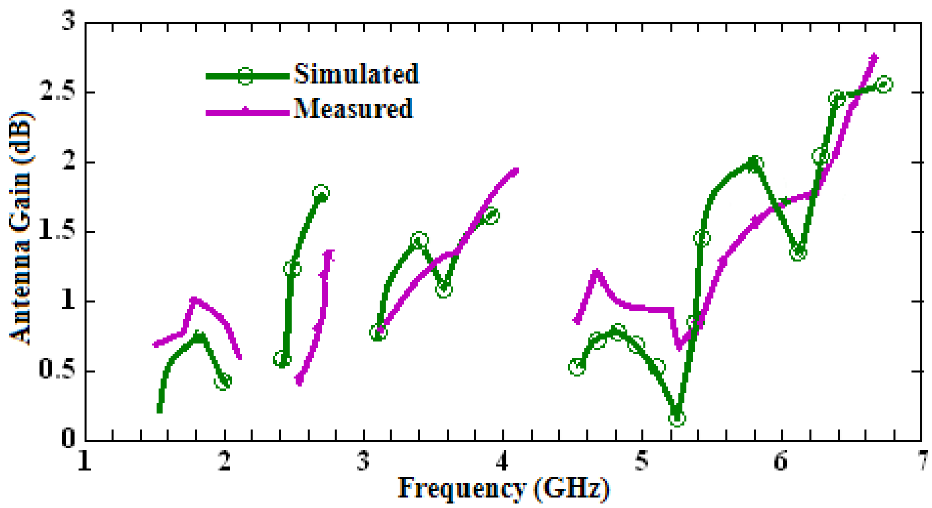

Figure 10. Simulated and measured gain of the proposed antenna.

Table 3. Comparison of the presented antenna with some other works.

Ref	Overall size (λc)	Feed method	Band Width (GHz)	Peak Gain (dBic)	AXBW (GHz)
[9]	$\lambda/3 \times \lambda/2 \times \lambda/40$	Microstrip	1.67-2.5, 5-6.14	~ 4	**n/a**
[10]	$\lambda/2 \times \lambda/3 \times \lambda/70$	Cpw	1.28-4.5	~ 5.3	**2.2-3.5**
[12]	$\lambda \times \lambda/2 \times \lambda/35$	Cpw	1.2-13	~ 3	**n/a**
[14]	$\lambda/4 \times \lambda/4 \times \lambda/55$	Cpw	2.28-2.48, 3.4-3.6	~ 2.9	**n/a**
[18]	$\lambda \times \lambda/2 \times \lambda/25$	Microstrip	1.61-17	~ 3.5	**n/a**
This work	$\lambda/3 \times \lambda/3 \times \lambda/55$	Microstrip	1.71-1.95, 2.42-2.73, 3.18-3.62, 4.45-5.31, 5.81-7.12	~ 2.75	**1.71-1.95, 2.42-2.75, 3.17-4.02, 4.25-5.25, 5.81-7.12**

Availability of data and materials
The data that support the findings of this study are available from the corresponding author upon reasonable request.

Conflict of interests
The authors declare that they have no known competing financial interests or personal relationships that could have appeared to influence the work reported in this paper.

References

[1] Y. JoongHan. "**Fabrication and measurement of modified spiral-patch antenna for use as a triple-band (2.4 GHz/5 GHz) antenna**.". 48(7):1275–1279, 2006.
DOI: https://doi.org/10.3103/S0735272716070050.

[2] J. Costantine, K. Y. Kabalan, A. El-Hajj, and M. Rammal. "**New multiband microstrip antenna design for wireless communications**.". *IEEE Trans. Antennas Propag. Mag.*, 49(6):181–186, 2007.
DOI: https://doi.org/10.1109/MAP.2007.4455895.

[3] S. C. Kim, S. H. Lee, and Y. S. Kim. "**Multi-band monopole antenna using meander structure for handheld terminals**.". *Electron. Lett.*, 44(5):331–332, 2008.
DOI: https://doi.org/10.1049/el:20080004.

[4] H. Wang and M. Zheng. "**Triple-band wireless local area network monopole antenna**.". *IET Microw. Antennas Propag.*, 2(4):367–372, 2008.
DOI: https://doi.org/10.1049/ic.2007.1084.

[5] C. H. See, R. A. Abd-Alhameed, P. S. Excell, N. J. McEwan, and J. G. Gardiner. "**Internal triple-band folded planar antenna design for third generation mobile handsets**.". *IET Microw. Antennas Propag.*, 2(7):718–724, 2008.
DOI: https://doi.org/10.1049/iet-map:2007035.

[6] H. C. Go and Y. W. Jang. "**Multi-band modified fork-shaped microstrip monopole antenna with ground plane including dual-triangle portion**.". *Electron. Lett.*, 40(10):575–577, 2004.
DOI: https://doi.org/10.1049/el:20040404.

[7] K. Seol, J. Jung, and J. Choi. "**Multi-band monopole antenna with inverted U-shaped parasitic plane**.". *Electron. Lett.*, 42(15): 844–845, 2006.
DOI: https://doi.org/10.1049/el:20061142.

[8] C. M. Wu, C. N. Chiu, and C. K. Hsu. "**A new nonuniform meandered and fork-type grounded antenna for triple-band WLAN applications**.". *IEEE Antennas Wirel. Propag. Lett.*, 5(1):346–348, 2006.
DOI: https://doi.org/10.1109/LAWP.2006.880692.

[9] W. C. Liu, M. Ghavami, and W. C. Chung. "**Triple-frequency meandered monopole antenna with shorted parasitic strips for wireless application**.". *IET Microw. Antennas Propag.*, 3(7):1110–1117, 2009.
DOI: https://doi.org/10.1049/iet-map.2008.0204.

[10] S. Das, H. Islam, T. Bose, and N. Gupta. "**Ultra wideband CPW-fed circularly polarized microstrip antenna for wearable applications**.". *Wirel.Pers. Commun.*, 108:87–106, 2019.
DOI: https://doi.org/10.1007/s11277-019-06389-9.

[11] M. R. Hasan, M. A. Riheen, P. Sekhar, and T. Karacolak. "**Compact CPW-fed circular patch flexible antenna for super-wideband applications**.". *IET Microw. Antennas Propag.*, 14:1069–1073, 2020.
DOI: https://doi.org/10.1049/iet-map.2020.0155.

[12] S. Lakrit, S. Das, S. Ghosh, and B. T. P. Madhav. "**Compact UWB flexible elliptical CPW-fed antenna with triple notch bandsfor wireless communications**.". *Int. J. RFMicrow. Comput. AidedEng.*, 30:e22201, 2020.
DOI: https://doi.org/10.1002/mmce.22201.

[13] T. Shanmuganantham, S. Ashok Kumar, and D. Sindhanaiselvi. "**C-SRR loaded CBCPW fed H-shaped slot radiator for ECG monitoring**.". *Int. J. Ultra-Wideband Commun.*, 5(2):96–102, 2022.
DOI: https://doi.org/10.1504/IJUWBCS.2022.123439.

[14] T. Shanmuganathan, S. Ashok Kumar, and S. Selvi. "**CB-CPW fed SRR loaded ISM and 5G low profile antenna for on-body healthcare monitor**.". *PIER-M*, 9:25–38, 2022.
DOI: https://doi.org/10.2528/PIERM22010701.

[15] J. P. Thakur and J. S. Park. "**An advance design approach for circular polarization of the microstrip antenna with unbalance DGS feedlines**.". *IEEE Antennas Wirel. Propag. Lett.*, 5(1):101–103, 2006.
DOI: https://doi.org/10.1109/LAWP.2006.872425.

[16] M. A. Antoniades and G. V. Eleftheriades. "**A compact multiband monopole antenna with a defected ground plane**.". *IEEE Antennas Wirel. Propag. Lett.*, 7:652–655, 2008.
DOI: https://doi.org/10.1109/LAWP.2008.2007813.

[17] K. H. Chiang and K. W. Tam. "**Microstrip monopole mntenna with enhanced bandwidth using defected ground structure**.". *IEEE Antennas Wirel. Propag. Lett.*, 7:532–535, 2008.
DOI: https://doi.org/10.1109/LAWP.2008.2005592.

[18] D. Nashaat, H. A. Elsadek, E. Abdallah, H. Elhenawy, and M. F. Iskander. "**Multiband and miniaturized inset feed microstrip patch antenna using multiple spiral-shaped defect ground structure (DGS)**.". *Proc. IEEE AP-S Int. Symp*, pages 1–4, 2009.
DOI: https://doi.org/10.1109/APS.2009.5171815.

[19] J. Pei, A-G. Wang, S. Gao, and W. Leng. "**Miniaturized triple-band antenna with a defected ground plane for WLAN/WiMAX applications**.". *IEEE Antennas Wirel. Propag. Lett*, 10:298–301, 2011.
DOI: https://doi.org/10.1109/LAWP.2011.2140090.

[20] A. Kumar, A. Q. Ansari, B. K. Kanaujia, and J. Kishor. "**Dual circular polarization with reduced mutual coupling among two orthogonally placed Cpw-fed microstrip antennas for broadband applications**.". *Wireless Personal Communication*, 107(2):759–770, 2019.
DOI: https://doi.org/10.1007/s11277-019-06298-x.

[21] A. Kumar, G. Saxena, P. Kumar, Y. K. Awasthi, P. Jain, S. S. Singhwal, and P. Ranjan. "**Quad-band circularly polarized super-wideband MIMO antenna for wireless applications**.". *Int. J. of RF and Microwave Computer-Aided Engineering*, 32(6):e23129, 2022.
DOI: https://doi.org/10.1002/mmce.23129.

[22] T. Sedgeechongaraluye-Yekan, R. A. Sadeghzadeh, and M. Naser-Moghadasi. "**Microstrip-fed circularly polarized antenna array using Semi-fractal cells for implicational band**.". *IETE Journal of Research*, 60(6):383–388, 2014.
DOI: https://doi.org/10.1080/03772063.2014.901484.

[23] T. Sedgeechongaralouye-Yekan, M. Naser-Moghadasi, and R. A. Sadeghzadeh. "**Broadband circularly polarized 2×2 antenna array with sequentially rotated feed network for C-band application**.". *Wireless Pers Commun*, 91:653–660, 2016.
DOI: https://doi.org/10.1007/s11277-016-3485-4.